

Effect of a photonic band gap on scattering from waveguide disorder

M. L. Povinelli,^{a)} Steven G. Johnson, Eleftherios Lidorikis, J. D. Joannopoulos, and Marin Soljačić

Department of Physics and the Center for Materials Science and Engineering, Massachusetts Institute of Technology, 77 Massachusetts Avenue, Cambridge, Massachusetts 02139

(Received 21 November 2003; accepted 20 February 2004; published online 20 April 2004)

We derive a general, analytical, coupled-mode theory for disorder-induced scattering in periodic systems that shows that in the experimentally relevant limit of weak disorder, the reflection in a photonic-crystal waveguide is just as low as in a comparable index-guided waveguide. Moreover, since the photonic band gap also blocks radiative loss, the total scattering loss is reduced, and the total transmission is higher. These general results are verified by direct numerical simulations in an example system. © 2004 American Institute of Physics. [DOI: 10.1063/1.1723686]

A photonic crystal blocks the propagation of fields within a certain frequency range, or photonic band gap, thereby confining light to the vicinity of defects in its periodic structure.¹ Linear defects, which act as waveguides, are promising building blocks for the design of optical integrated circuits in photonic crystals.² Understanding the effects of disorder in these systems (e.g., from imperfect fabrication) is thus a topic of both fundamental and practical importance. However, while the effect of disorder on the bulk band gap of the crystal is well understood,^{3,4} the effect of disorder on transport through photonic-crystal waveguides has seen only limited study for specific cases.^{5–8}

In this letter, we derive the general principles that govern scattering due to arbitrary disorder in photonic-crystal waveguides. Using a basis of Bloch states, we develop an extension of coupled-mode theory⁹ valid for strongly periodic, high-index-contrast systems. Unlike previous work, our approach is not limited to slowly varying perturbations,¹⁰ develops the coupled-mode equations in space rather than in time,¹¹ and uses a fixed basis.¹² From the theory, an explicit formula for reflection is obtained, yielding insight into the effect of the band gap on scattering. We find that, in the experimentally relevant limit of weak disorder,¹³ the photonic band gap suppresses radiation loss *without* redirecting light into reflection. As a result, reflection losses are the same as in a comparable index-guided waveguide, and overall transmission is higher. These general results are verified by direct simulations of Maxwell's equations in an example system.

We begin by writing the dielectric constant of the waveguide as $\varepsilon(x,y,z) + \Delta\varepsilon(x,y,z)$, corresponding to a z -periodic, unperturbed waveguide ε of period a plus a perturbation $\Delta\varepsilon$ due to disorder, where z is the propagation direction. For a definite frequency ω , the fully vectorial source-free Maxwell's equations can be rewritten as¹³

$$(\hat{A} + \Delta\hat{A})|\psi\rangle = -i \frac{\partial}{\partial z} \hat{B}|\psi\rangle,$$

where $|\psi\rangle$ is a four-component column vector containing the transverse (xy) fields \mathbf{E}_t and \mathbf{H}_t ,

$$|\psi\rangle \equiv \begin{pmatrix} \mathbf{E}_t(x,y,z) \\ \mathbf{H}_t(x,y,z) \end{pmatrix} e^{-i\omega t},$$

$$\hat{A} \equiv \begin{pmatrix} \frac{\omega\varepsilon}{c} - \frac{c}{\omega} \nabla_t \times \frac{1}{\mu} \nabla_t \times & 0 \\ 0 & \frac{\omega\mu}{c} - \frac{c}{\omega} \nabla_t \times \frac{1}{\varepsilon} \nabla_t \times \end{pmatrix},$$

$$\Delta\hat{A} = \begin{pmatrix} \omega\Delta\varepsilon/c & 0 \\ 0 & -\frac{c}{\omega} \nabla_t \times \Delta\left(\frac{1}{\varepsilon}\right) \nabla_t \times \end{pmatrix},$$
(1)

where $\Delta(1/\varepsilon) = -\Delta\varepsilon/[\varepsilon(\varepsilon + \Delta\varepsilon)]$, and

$$\hat{B} \equiv \begin{pmatrix} 0 & -\hat{\mathbf{z}} \times \\ \hat{\mathbf{z}} \times & 0 \end{pmatrix}.$$

∇_t denotes transverse (xy) components of ∇ . In contrast to quantum mechanics, \hat{A} and \hat{B} are Hermitian (for real ε , μ) but not positive definite, allowing complex eigenvalues.

From Bloch's theorem, the eigenstates of the unperturbed system can be written $e^{i\beta z}|\beta\rangle$, where the real part of $\beta \in (-\pi/a, \pi/a]$, and $|\beta\rangle$ is a z -periodic function with period a that satisfies the generalized Hermitian eigenproblem

$$\left(\hat{A} + i \frac{\partial}{\partial z} \hat{B}\right)|\beta\rangle = \beta \hat{B}|\beta\rangle.$$
(2)

The orthogonality condition is $\langle\beta^*|\hat{B}|\beta'\rangle = 0$ for $\beta \neq \beta'$, where $|\beta^*\rangle$ is the eigenstate with eigenvalue β^* , and the implicit integral is over one unit cell. (Modes with complex β are evanescent.) While a complete basis at constant ω includes a continuum of nonguided states, this continuum can be regarded as the infinite-volume limit of the set of discrete states of a finite volume with conducting boundary conditions. We thus consider only modes $|n\rangle$ that have discrete eigenvalues β_n , normalized such that $\langle m^*|\hat{B}|n\rangle = \delta_{m,n}\eta_n$ with $|\eta_n| = 1$; moreover, $\langle m^*|\hat{B}e^{(-2\pi i/a)\ell z}|n\rangle = 0$ for $\beta_m \neq \beta_n + (2\pi/a)\ell$.

Because the orthonormality condition involves an integral over the unit cell, it is useful to adopt an algebraic trick¹² to introduce a new integration parameter \tilde{z} , a shift of the original, unperturbed waveguide. Consider

^{a)}Electronic mail: mpovinel@alum.mit.edu

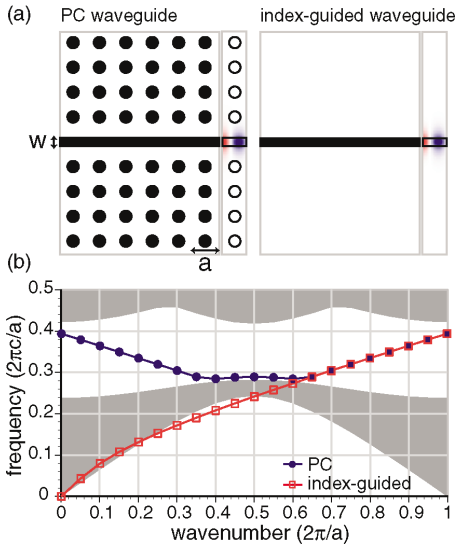


FIG. 1. (Color) (a) Waveguide geometries and mode profiles for $\omega = 0.31(2\pi c/a)$. Mode profiles show the electric field component perpendicular to the page; red and blue indicate negative and positive values, respectively. (b) Band diagram for the waveguides shown in (a). Shaded regions indicate extended TM states of the bulk 2D photonic crystal.

$$(\hat{A}(z+\tilde{z}) + \Delta\hat{A})|\psi\rangle_{\tilde{z}} = -i \frac{\partial}{\partial \tilde{z}} \hat{B}|\psi\rangle_{\tilde{z}}, \quad (3)$$

where $\hat{A}(z+\tilde{z})$ is obtained by sending $\epsilon(x,y,z) \rightarrow \epsilon(x,y,z+\tilde{z})$ in Eq. (1). The solution of Eq. (3) can be expanded as

$$|\psi(z)\rangle_{\tilde{z}} = \sum_n c_n(z,\tilde{z})|n(z+\tilde{z})\rangle e^{i\beta_n z}. \quad (4)$$

Since $\hat{A}(z+\tilde{z}+a) = \hat{A}(z+\tilde{z})$, the c_n 's can be chosen to be periodic in \tilde{z} and expressed as a Fourier series:

$$c_n(z,\tilde{z}) = \sum_{\ell} c_{n,\ell}(z) e^{-2\pi i \ell \tilde{z}/a}. \quad (5)$$

After substituting Eq. (4) into Eq. (3), using a shifted version of Eq. (2) for the shifted, unperturbed eigenstates $|n(z+\tilde{z})\rangle$, and applying a \tilde{z} -shifted orthonormality condition, the physical solution is obtained by setting \tilde{z} to zero.

After integration by parts and a change of variables, the final result is¹⁴

$$\begin{aligned} \frac{dc_m}{dz} \Big|_z &= i \eta_m^* \sum_{k,n,\ell} c_{n,\ell}(z) e^{i(\beta_n - \beta_m + 2\pi(\ell-k)/a)z} \\ &\times \int d\mathbf{x}' e^{-2\pi i(\ell-k)z'/a} \frac{\omega}{c} \left[\Delta\epsilon(\mathbf{x}',z) \mathbf{E}_t^{m*}(\mathbf{x}')^* \right. \\ &\left. \cdot \mathbf{E}_t^n(\mathbf{x}') - \Delta \left(\frac{1}{\epsilon(\mathbf{x}',z)} \right) D_z^{m*}(\mathbf{x}')^* D_z^n(\mathbf{x}') \right], \quad (6) \end{aligned}$$

where $\mathbf{E}_t \equiv e^{i\beta_n z} \mathbf{E}_t^n$. Note that the integral is over $\mathbf{x}' = (\mathbf{x}', z')$, which ranges over the unit cell, whereas z is the fixed point along the waveguide axis at which dc_m/dz is evaluated. From Eq. (6) it can be seen that mode coupling depends on the strength of the perturbation at a given z and a weighted average of the mode profiles over the *entire* unit cell. Assuming for simplicity that the unperturbed waveguide is single-mode, the coupled-mode equations can be integrated to first order to yield the reflection coefficient:

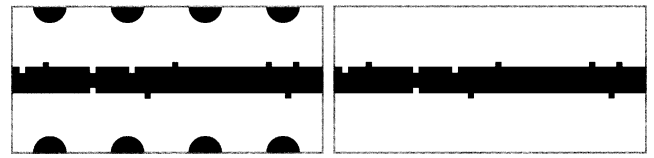


FIG. 2. Closeup of central waveguide region, showing how identical surface roughness was added to the photonic-crystal and index-guided waveguides.

$$\begin{aligned} c_r(z) &\approx -i \sum_k \int dz e^{i(2\beta_i - 2\pi k/a)z} \int d\mathbf{x}' e^{2\pi i k z'/a} \frac{\omega}{c} \\ &\times \left(\Delta\epsilon(\mathbf{x}',z) \mathbf{E}_t^i(\mathbf{x}')^* \cdot \mathbf{E}_t^j(\mathbf{x}') \right) \\ &- \Delta \left(\frac{1}{\epsilon(\mathbf{x}',z)} \right) D_z^i(\mathbf{x}')^* D_z^j(\mathbf{x}') \Big) c_i(0), \quad (7) \end{aligned}$$

where i/r label incident/reflected modes. (A factor of $\sqrt{1/v_g}$ is implicit in the mode normalization.¹²)

Equation (7) shows that for weak-disorder, a photonic band gap surrounding the waveguide has *no effect* on reflection. To first order, only the profiles of the guided modes enter the formula for the reflection coefficient, along with the dispersion relation $\beta(\omega)$, the group velocity v_g , and the perturbation $\Delta\epsilon$. As a result, a photonic-crystal waveguide with weak disorder will have the *same* reflection losses as an index-guided waveguide that shares these characteristics, regardless of the guiding mechanism. Moreover, the total transmission will be higher for the photonic-crystal waveguide, since the index-guided waveguide suffers additional radiative losses.¹⁵ It is natural to suppose that reflection losses might be higher for a photonic-crystal waveguide than for an index-guided waveguide, for one could imagine that the suppression of radiative scattering loss by the photonic crystal would redirect light into reflection (as well as in the forward direction). However, to first order, redirection does not occur. Because the photonic crystal modifies the local density of states at the scattering site, the *total* scattered power is *lower*, and the total reflected power is the same as in a comparable index-guided waveguide.

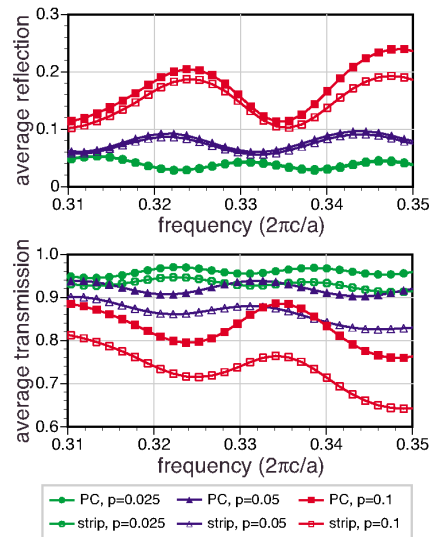


FIG. 3. (Color) Transmission and reflection for a disordered region of length $10a$, averaged over 20 realizations of the disorder.

As a specific illustration, consider the waveguides in Fig. 1(a). On the left is a two-dimensional (2D) photonic-crystal (PC) waveguide made by introducing a high-index strip of width w into the center of a missing row of rods.^{16,17} The bulk crystal is composed of a 2D array of high-index rods in air. On the right is a waveguide composed of the high-index strip alone. A comparison of the two systems provides a clear demonstration of the effect of a photonic band gap on disorder-induced scattering, because their *only* difference is the presence of the band gap.

Figure 1(b) shows the dispersion relations of both structures computed by plane wave expansion,¹⁸ for rod radius $r = 0.2a$, $w = 0.3a$, and $\epsilon = 12$. Shaded regions indicate extended TM states of the bulk 2D photonic crystal. Filled, blue circles show the PC waveguide mode, which traverses the band gap. Open, red squares show the fundamental mode of the index-guided waveguide. The dispersion relations coincide for wave numbers β greater than $\sim 0.65(2\pi/a)$. In this range, the electric field profiles are nearly identical; Fig. 1(a) shows the electric field perpendicular to the paper for $\omega = 0.31(2\pi c/a)$. Quantitatively, the unit-cell average of $|E_x|^2$ at the waveguide surface is the same to within 0.1%. Equation (7) predicts the two waveguides will have nearly identical reflection in the weak-disorder limit.

Surface roughness was added to both waveguides, and the reflection and transmission were calculated using 2D, full-vectorial, finite-difference time domain simulations of Maxwell's equations.¹⁹ The computational resolution was 20 grid points/ a . Perfectly-matched-layers were used at the boundaries of the computational cell.²⁰ Figure 2 shows the central waveguide region. For each realization of disorder, the same perturbation was made to both waveguides. Along each side of the strip, a random perturbation was made at each grid point, with a probability p of a pixel being added and p of being removed. No perturbation was made to the rod surfaces. Aside from a slight narrowing of the band gap,^{3,4} the effect of such a perturbation is negligible for weak disorder. Because the mode is strongly localized in the central strip, scattering is dominated by roughness along the strip surfaces.

Figure 3 shows reflection and transmission as a function of frequency, where the results are averaged over 20 realizations of disorder and the length L of the disordered segment is $10a$. For the frequency range shown, the dispersion relations of the two waveguides overlap (see Fig. 1). Results are plotted for three values of the disorder probability. At the highest value, $p = 0.1$, the reflection in the PC waveguide is higher than in the strip waveguide by 2%–6% due to second-order scattering. As p is decreased, the difference in reflection decreases and is unobservable for $p = 0.025$. For all three values of p , the transmission through the PC waveguide is higher than for the index-guided waveguide. The oscillations in the frequency spectrum visible in both average reflection and transmission are due to Fabry–Perot effects arising from the finite length of the disordered region. The period of oscillation corresponds to $L \sim 10a$ and was found to scale linearly with L ; the magnitude of the oscillations decreases linearly with p .

Average transmission through the PC waveguide decreases more slowly with length than for the index-guided

waveguide. For $p = 0.05$, the calculated losses were ~ 0.04 dB/ a (PC) and ~ 0.07 dB/ a (index-guided waveguide).

While the numerical results we present are for a specific, 2D system, the coupled-mode theory developed here provides a general, semi-analytical framework that can be used to study the effects of arbitrary disorder in a variety of three-dimensional photonic crystals. Moreover, the physical insight gained applies to general photonic-crystal waveguides: in the limit of weak disorder, the photonic crystal suppresses radiation loss without redirecting light into reflection. The results should be of interest for the development of low-loss waveguides in high to medium index contrast systems using photonic crystals with full or partial band gaps. Several avenues for future study include the direct semi-analytical prediction of disorder losses in realistic systems and the development of a generalized coupled-power theory⁹ based on Eq. (6). The latter can be used to illuminate the effects of long-correlation-length ($\gg a$) disorder, which may cause additional scattering/reflection due to quasiphase matching, as well as to allow comparison of photonic-crystal waveguides that do not directly correspond to conventional waveguides.

This work was supported in part by the Materials Research Science and Engineering Center program of the NSF under Award No. DMR-9400334. The authors thank A. Vishwanath, D. Kielpinski, Y. S. Kivshar, S. J. Spector, M. W. Geis, T. M. Lyszczarz, S. Assefa, M. P. Brenner, and E. P. Ippen for useful discussions.

¹J. D. Joannopoulos, R. D. Meade, and J. N. Winn, *Photonic Crystals: Molding the Flow of Light* (Princeton University Press, New York, 1995).

²T. F. Krauss, *Phys. Status Solidi A* **197**, 688 (2003).

³E. Lidorikis, M. M. Sigalas, E. N. Economou, and C. M. Soukoulis, *Phys. Rev. B* **61**, 13458 (2000).

⁴A. A. Asatryan, P. A. Robinson, L. C. Botten, R. C. McPhedran, N. A. Nicorovici, and C. M. de Sterke, *Phys. Rev. E* **62**, 5711 (2000).

⁵K.-C. Kwan, X. Zhang, Z.-Q. Zhang, and C. T. Chan, *Appl. Phys. Lett.* **82**, 4414 (2003).

⁶B. Z. Steinberg, A. Boag, and R. Lisitsin, *J. Opt. Soc. Am. A* **20**, 138 (2003).

⁷W. Bogaerts, P. Bienstman, and R. Baets, *Opt. Lett.* **28**, 689 (2003).

⁸T. N. Langtry, A. A. Asatryan, L. C. Botten, C. M. de Sterke, R. C. McPhedran, and P. A. Robinson, *Phys. Rev. E* **68**, 026611 (2003).

⁹D. Marcuse, *Theory of Dielectric Optical Waveguides*, 2nd ed. (Academic, San Diego, 1991).

¹⁰P. St. J. Russell, *Phys. Rev. Lett.* **56**, 596 (1986).

¹¹C. M. de Sterke, D. G. Salinas, and J. E. Sipe, *Phys. Rev. E* **54**, 1969 (1996).

¹²S. G. Johnson, P. Bienstman, M. A. Skorobogatiy, M. Ibanescu, E. Lidorikis, and J. D. Joannopoulos, *Phys. Rev. E* **66**, 066608 (2002).

¹³Typical experimental magnitudes of roughness due to lithography (Refs. 2 and 21) will be even lower than those we study here.

¹⁴The result must be modified using techniques discussed in (Ref. 22) for boundary perturbations with non-TM modes.

¹⁵The lowest order correction to the power transmission is $T(z) = 1 - |c_r(z)|^2 - \sum_{m \neq i, r} |c_m(z)|^2$, where the sum includes radiative terms similar to Eq. (7).

¹⁶S. G. Johnson, P. R. Villeneuve, S. Fan, and J. D. Joannopoulos, *Phys. Rev. B* **62**, 8212 (2000).

¹⁷W. T. Lau and S. Fan, *Appl. Phys. Lett.* **81**, 3915 (2002).

¹⁸S. G. Johnson and J. D. Joannopoulos, *Opt. Express* **8**, 173 (2001).

¹⁹K. S. Kunz and R. J. Luebbers, *The Finite-Difference Time-Domain Method for Electromagnetics* (CRC Press, Boca Raton, FL, 1993).

²⁰J. C. Chen and K. Li, *Microwave Opt. Technol. Lett.* **10**, 319 (1995).

²¹K. K. Lee, D. R. Lim, H.-C. Luan, A. Agarwal, J. Foresi, and L. C. Kimerling, *Appl. Phys. Lett.* **77**, 1617 (2000).

²²S. G. Johnson, M. Ibanescu, M. Skorobogatiy, O. Weisberg, J. D. Joannopoulos, and Y. Fink, *Phys. Rev. E* **65**, 066611 (2002).